Project PAJex1 - Report 3

Strength of Adhesive Joints: A Parametric Study

W R Broughton, L E Crocker and J M Urquhart

July 2001

NPL Materials Centre
National Physical Laboratory
NPL Report MATC(A)27

NPL

NPL Report MATC(A)27
July 2001

Strength of Adhesive Joints: A Parametric Study

W R Broughton, L E Crocker and J M Urquhart
NPL Materials Centre
National Physical Laboratory
Teddington, Middlesex
TW11 0LW, UK

ABSTRACT

A parametric study has been carried out to assess the reliability of different failure criteria being used by engineers / designers to predict the static strength of adhesively bonded structures. A series of simulated experiments using finite element analysis (FEA) have been conducted on single-lap and scarf joint configurations for this purpose. The FEA was used to establish the effects of specimen geometry and different elastic-plastic material models on stress and strain distributions within the adhesive layer, and the joint strength. Von Mises and linear Drucker-Prager materials models were used characterise deformation behaviour of the adhesive. Algebraic formulations relating geometric parameters to joint strength were derived using statistical analysis (Design of Experiments). Experimental results were used to validate the analysis procedure.

The results from the parametric study demonstrate that joint strength for the two geometries can be determined, to a reasonable degree of accuracy, using a two-dimensional finite element modelling approach in conjunction with suitable failure criteria, provided that plasticity of the adhesive and adherends is taken into account. The study also revealed that the stress and strain distributions, and hence failure, for the two joint configurations are sensitive to changes in adhesive layer thickness, adherend thickness, bond length and taper angle (scarf joint only).

The report was prepared as part of the research undertaken at NPL for the Department of Trade and Industry funded project on "Performance of Adhesives Joints Extension (PAJex) Programme– Deformation and Failure of adhesive Joints".

ISSN 1473 - 2734

National Physical Laboratory
Teddington, Middlesex, UK, TW11 0LW

Approved on behalf of Managing Director, NPL, by Dr C Lea,
Head of NPL Materials Centre.

CONTENTS

1 INTRODUCTION 1

2 FAILURE CRITERIA 1

2.1 STRENGTH OF MATERIALS BASED MODELS 2

2.2 PLASTIC YIELD CRITERIA 2

2.3 VOID NUCLEATION (CAVITATION) MODELS 4

2.4 FRACTURE MECHANICS 5

3 NUMERICAL MODELLING 6

3.1 SINGLE-LAP JOINT 6

3.2 SCARF JOINT 10

4 SINGLE-LAP JOINT ANALYSIS 11

4.1 FAILURE CRITERIA 11

4.2 ANALYTICAL ANALYSIS 12

4.3 NUMERICAL RESULTS 13

4.4 DISCUSSION 16

5 SCARF JOINT ANALYSIS 17

5.1 ANALYTICAL ANALYSIS 17

5.2 NUMERICAL RESULTS 18

6 DISCUSSION AND CONCLUDING REMARKS 22

ACKNOWLEDGEMENTS 23

REFERENCES 23

APPENDICES 25

1 INTRODUCTION

Altering the geometry of a bonded joint will invariably alter the stress and strain distributions within the adhesive layer [1-2]. These differences have a profound affect on the stress concentrations and consequently the load-capacity of the joint. It is therefore important to appreciate the consequences of changing geometric and material parameters. In order to predict failure (i.e. cohesive failure in the adhesive layer) loads, a criterion is needed that will define when a critical level of stress or strain is reached in the adhesive to initiate rupture. This failure (or yield) criterion can be used, in conjunction with calculated stress and strain distributions within the critical regions of the bond, to predict the onset and progression of failure of the joint.

This report presents the results of a parametric study that was carried out to evaluate the ability of commonly used failure criteria for predicting the static strength of rubber-toughened adhesive joints. Finite element analysis (FEA) was used to establish the effects of these parameters on the joint stiffness, stress and strain distributions within the adhesive layer, and joint strength. A series of simulated experiments using FEA were conducted on single-lap and scarf joints to determine the effects of adhesive layer (bondline) thickness, adherend thickness and bond length, and taper angle in the case of scarf joints, for this purpose. Von Mises and linear Drucker-Prager materials models were used characterise deformation behaviour of the adhesive. Statistical analysis (Design of Experiments) has been used to derive simple mathematical relationships for determining the effects of geometric parameters on joint strength. The validity of the failure criterion has been assessed by comparing with experimental data from tests conducted on the single-lap and scarf joints.

The report is divided into six (6) sections (including Section 1, Introduction). Section 2 presents an overview of criteria for predicting the cohesive strength of adhesives and adhesively bonded structures. Section 3 covers the numerical modelling of the single-lap and scarf joint geometries using FEA. The effects of geometric and material parameters on single-lap and scarf joint performance are considered in Sections 4 and 5, respectively. Conclusions and discussion are given in Section 6.

The research discussed in this report forms part of the Engineering Industries Directorate of the United Kingdom Department of Trade and Industry project PAJex1 “Performance of Adhesive Joints – Deformation and Failure of Toughened Adhesives”.

Throughout this report, statements of particular importance or relevance are highlighted in bold type.

2. FAILURE CRITERIA

A number of approaches, listed below, have been adopted by engineers / designers for predicting the static strength (failure load) of adhesives and adhesively bonded structures.

(i) Strength of materials based models (e.g. average stress, maximum stress and maximum strain failure criterion) [3-10];

(ii) Plastic yield criteria (e.g. von Mises and Tresca yield criterion, and Drucker-Prager plasticity model) [11-15];

(iii) Void Nucleation (Cavitation) models [16-18]; and

(iv) Fracture-mechanics analysis [19-27].

2.1 STRENGTH OF MATERIALS BASED MODELS

A number of strength of materials based models have been proposed for predicting the strength of bulk adhesives and adhesively bonded joints [3-10]. These include:

Average Stress Method: This approach assumes that the strength of the joint is equal to the average shear or normal stress in the adhesive layer at the point of failure (i.e. maximum load). For a single-lap joint configuration, the average shear stress is given by [8]:

$$\tau = \frac{P}{bl} \tag{1}$$

where **P** is the applied load, **b** is the joint width and **l** is the bond length.

The average stress method is unable to account for out-of-plane deformation associated with the eccentricity of the load path and the flexibility of the adhesive and the adherends. The analysis is too simplistic, it assumes the adherends are rigid, and that the adhesive only deforms in shear. In fact, the resultant stress distribution, across and along the bond length is very complex and is dependent on adhesive and adhesive properties, and joint geometry. Failure results from the combined action of peel and shear stress and strain concentration present at the ends of the adhesive joint.

Maximum Stress Method: This approach, which is widely used in industry, compares the maximum stress in the adhesive layer (normal, shear or von Mises) with the tensile, compressive or shear strength of the adhesive. Failure is deemed to have occurred when the stress exceeds one of the strength values. This approach allows for non-uniform stress distributions along the bond length and through the thickness of the adhesive. Analytical (closed-form equations) or FEA can be used to determine the stress distributions within the adhesive layer. For many applications, closed-form analysis is not feasible for modelling the stress and strain distributions within the adhesive, and hence FEA tends to be used to predict the deformation and strength of bonded structures. A major limitation with FEA is the inability to account for points of stress singularity, such as those present at the ends of bonded joints. The FEA results depend on the element size with the value of the stresses increasing as the element size near the singularity is reduced. If stresses become infinite, then the predicted load at failure is zero. It has been suggested that the element size in regions of high stress gradients be equal to one third of the adhesive thickness [9].

Maximum Strain Criterion: According to Hart-Smith [3-6], maximum lap-joint strength is defined by the adhesive strain energy in shear (i.e. stress level for joint failure is mainly dependent on the shear strain to failure of the adhesive). A maximum strain criterion proposed by the Hart-Smith is now widely used within the aerospace industry for determining strength of metallic and composite joints. The analysis developed by Hart-Smith [4, 6] accounts for non-linear elastic-plastic deformation in the adhesive.

2.2 PLASTIC YIELD CRITERIA

The strength of materials based models considered above tend to assume that the adhesive behaves as a linear-elastic solid (i.e. no plasticity). However, many adhesives (e.g. rubber-modified epoxies) exhibit large plastic strains to failure. A number of theoretical criteria

have been proposed for describing the yield behaviour of polymers under multi-component stress states. These include Tresca yield and von Mises yield criteria, and Drucker Prager plasticity model [11-15].

Tresca Yield Criterion: This criterion was initially developed to describe the yield behaviour of metals. Tresca proposed that yield occurs when the maximum shear stress, τ_{max}, reaches a critical value. If $\sigma_1 > \sigma_2 > \sigma_3$ (principal stress components in the 1-, 2- and 3- orthogonal directions) then the criterion is given as [11, 13]:

$$\tau_{max} = \frac{1}{2}(\sigma_1 - \sigma_3) \tag{2}$$

σ_1 and σ_3 are the maximum and minimum principal stresses, respectively.

In the case of simple tension:

$$\tau_{max} = \frac{\sigma_1}{2} = \frac{\sigma_y}{2} \tag{3}$$

where σ_y is the yield stress in tension.

The Tresca yield criterion is unable to accurately model the behaviour of rubber-toughened adhesives under tensile, compressive or shear loads; as yielding in these materials is sensitive to hydrostatic stress. In response, the Tresca yield criterion has been modified to include the effect of hydrostatic stress. The modified criterion states that the maximum shear stress, τ_{max}, is related to the yield stress in pure shear, τ^o, hydrostatic pressure, **p** and the pressure sensitivity of the adhesive, μ_t.

$$\tau_{max} = \tau^o + \mu_t p \tag{4}$$

where the hydrostatic pressure, **p**, is expressed in terms of triaxial stresses σ_1, σ_2 and σ_3.

$$p = -\frac{\sigma_1 + \sigma_2 + \sigma_3}{3} \tag{5}$$

The maximum shear stress, τ_{max}, is expressed in terms of the maximum and minimum principal stresses (see Equation (2)).

Von Mises Yield Criterion: In this criterion, yield occurs when the shear strain energy in the material reaches a critical value. The critical strain energy value is expressed in terms of the principal stresses by the following symmetric relationship [11, 13]:

$$(\sigma_1 - \sigma_2)^2 + (\sigma_2 - \sigma_3)^2 + (\sigma_3 - \sigma_1)^2 = \text{constant} \tag{6}$$

In the case of simple tension:

$$(\sigma_1 - \sigma_2)^2 + (\sigma_2 - \sigma_3)^2 + (\sigma_3 - \sigma_1)^2 = 2\sigma_y^2 \tag{7}$$

In the case of pure shear, the shear yield stress is predicted to be:

$$\sigma_1 = \sigma_y / \sqrt{3} \tag{8}$$

The von Mises yield criterion, however cannot accurately model the behaviour of rubber-toughened bulk adhesive specimens under tensile, compressive or shear loads; as yielding in these materials is sensitive to hydrostatic as well as the shear stress [15]. The von Mises yield criterion has been modified to account for the combined effect of these stresses, and can mathematically be described as follows [14]:

$$\tau_{max} = \tau_m^o + \mu_m p \tag{9}$$

where t_m denotes the von Mises yield stress, which is defined by the following equation:

$$6\tau_m^2 = (\sigma_1 - \sigma_2)^2 + (\sigma_2 - \sigma_3)^2 + (\sigma_3 - \sigma_1)^2 \tag{10}$$

and τ_m^o is the yield stress in pure shear. The parameter m_m can be determined from stress / strain measurements under two different stress states.

If tension and shear stress / strain curves are available, m_m can be determined as follows:

$$\mu_m = 3\left[\left(\sqrt{3}\sigma_S / \sigma_T\right) - 1\right] \tag{11}$$

where s_S and s_T are yield stresses at the same effective plastic strain. Alternatively, if curves from compression and shear tests are available, m_m can be determined as follows:

$$\mu_m = 3\left[1 - \left(\sqrt{3}\sigma_S / \sigma_C\right)\right] \tag{12}$$

where s_S is the shear yield stress at the same effective plastic strain as s_C.

Alternative criterion, such as the Drucker-Prager plasticity model, has been used to model the yield behaviour of adhesives with limited success [14-15]. The Drucker-Prager model was developed for determining the pressure dependent yield failure of soils (i.e. porous materials). As with the Tresca and von Mises yield criteria, Drucker-Prager criterion is unable to characterise the yield surface for rubber-toughened epoxy adhesives and over predicts the effect of compressive hydrostatic stress on yielding. Recently, the Drucker-Prager model has been mathematically modified to account for both tensile and compressive hydrostatic stresses [14].

2.3 VOID NUCLEATION (CAVITATION) MODELS

Plastic yield criteria, described in Section 1.3, assume that the onset of non-linear behaviour arises from plastic deformation. At the first yield point, there is a reduction in true stress (a region where the stress rises less steeply than the strain). This reduction in true stress is attributed to “strain softening”. Subsequent increases of stress with strain are attributed to strain hardening (see [9, 14]). However, elastic-plastic models do not allow for the effects of rubber particle cavitation on the yield and plastic deformation in which there is a dilatational component in the stress tensor. For rubber-toughened adhesives, the generation and growth

of cavities within the rubber particles enhances plastic deformation of the material when subjected to dilatational stress states. The cavitation produces an increase in stress concentration, enabling the material to dilate through the growth of voids (made possible through matrix shear yielding) [14].

A number of models have been proposed, which attempt to account for the effect of void nucleation on ductility [16]. Gurson [17] developed a yield criterion and flow rule for a material containing a given volume fraction of voids. Bucknall and co-workers [18-19] have considered rubber-toughened polymers and proposed that rubber particle cavitation occurs at a critical volumetric strain that depends on the radius and elastic modulus of the rubber particles, and surface energy. The authors modified Gurson's yield criterion to incorporate a term to allow for the pressure dependence of the yield stress for uncavitated polymer matrix.

Dean and co-workers at the National Physical laboratory [16] have modified Gurson's yield criterion to include a void nucleation function relating the void fraction to the applied volumetric strain. The modified criterion allows for the changing composition of the polymer matrix during void nucleation. The model has been shown to predict the stress/strain response of bulk adhesives in tension and compression, and adhesively bonded tensile-butt joints. Mathematical details of the model can be obtained in reference [16].

2.4 FRACTURE MECHANICS

The fracture mechanics approach assumes a pre-existent crack and uses FEA to determine the stress state in the vicinity of the crack tip. It is worth noting that good progress has been made in applying fracture mechanics to predicting crack growth and failure of adhesively bonded joints for single-mode loading configurations [20-27], although the relevance and potential usage to actual bonded structures is regarded by the engineering community with some scepticism.

From an engineering perspective, prediction of crack growth rate is considered less important than determining the crack initiation stress or energy. Nonetheless, a considerable amount of effort has been expended in attempting to predict crack initiation and the rate of crack growth in adhesively bonded joints (e.g. tapered double cantilever beam and single-lap) subjected to mode I (tension), mode II (shear) and mode I/II static and cyclic loading conditions. A number of these investigators [20-27] have found good correlation between strain energy release rates and joint fracture.

The approach is best suited to predicting failure subsequent to fracture propagation along a parallel crack path. However, failure is often catastrophic with no visible evidence of crack growth prior to the onset of failure. In these cases, failure is controlled primarily by the initial size of defects or flaws present in regions of high stress gradients (e.g. adhesive fillets). It has been suggested that failure occurs when the maximum stress/strain exceeds a critical stress/strain value at a distance, or when the stress acting over a certain volume exceeds a critical value [27].

The critical distance or volume, which is generally defined using FEA and experimental data, is a function of the specimen geometry and size, and the defect spectrum contained within the specimen. The adhesive in regions of high-localised stresses (e.g. joint fillets) may be intrinsically stronger than bulk adhesive test specimens because the former is less likely to contain a critical flaw. Weibull statistical analysis has been used to model the sensitivity of

both distance and volume failure criteria to changes in local geometry and singularity strength (see [27]).

3. NUMERICAL MODELLING

This section discusses the FEA that was carried out on two joint configurations to assess the accuracy (or reliability) of existing failure criteria for predicting joint strength. A series of simulated experiments using FEA have been conducted on single-lap and scarf joint configurations for this purpose. Ideally, the failure criterion should apply equally to all test geometries; independent of specimen dimensions. FEA was used to investigate the effect of the following parameters on the joint strength.

- Adherend thickness (single-lap joint)
- Adhesive thickness (single-lap and scarf joints)
- Bond (or overlap) length (single-lap joint)
- Fillet geometry (single-lap)
- Taper angle (scarf joint)

The materials used for this study were mild steel adherends bonded with AV119 (Araldite® 2007) a single part epoxy adhesive (supplied by Vantico) or XD4601 a single-part, toughened epoxy adhesive (supplied by Essex Betamate). Both epoxy adhesives are high temperature curing systems.

The FE models presented in this report were constructed and solved using ABAQUS [28] program while mesh generation was performed using FEMGV [29] pre-processor. Two elastic-plastic materials models, von Mises and Linear Drucker-Prager, were used with the FEA to predict the deformation behaviour of the two joint configurations.

3.1 SINGLE-LAP JOINT

Although, a converged three-dimensional analysis may provide a more accurate solution to the problem of structural assessment of adhesive joints than two-dimensional analysis, the time and effort required for mesh generation and analysis of results is substantially increased. Two-dimensional analysis is generally preferred for comparative studies where a series of finite element models are required. **However, the assumptions of plane stress or plane strain will not be valid at all locations within the joint**. Stiffness changes in the width direction cannot be modelled.

A two-dimensional finite element model was constructed to determine the stress and strain distributions in a single-lap joint and to carry out the parametric evaluation of key geometric variables [2]. The bond between the adherend and the adhesive was assumed to be perfect with the adhesive and interface free of defects (i.e. voids). Both the adhesive and adherend were represented by plane strain isoparametric elements.

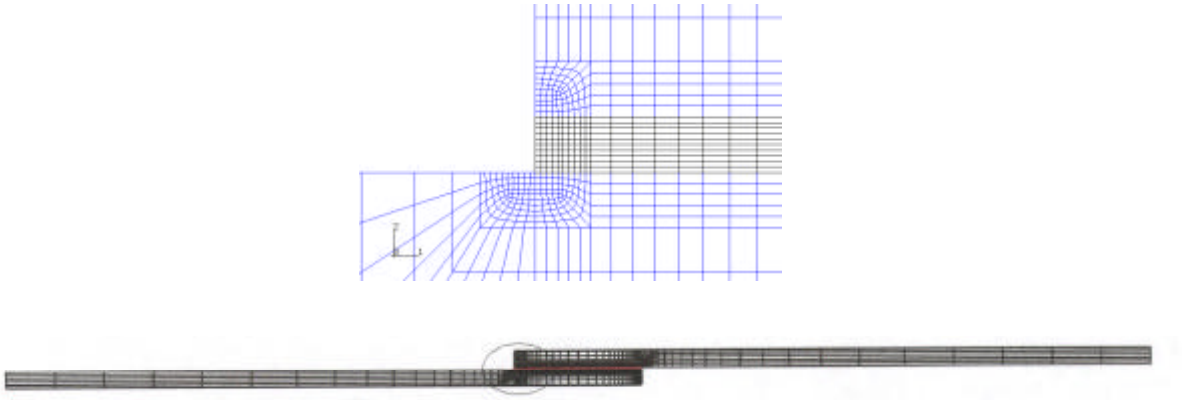

Figure 1: Two-dimensional finite element mesh for single-lap joint.

The constraints and loads were applied so as to mimic the tensile loading conditions on the specimen while it was secured in non-rotating clamps. The load was applied along the 1-axis as "a distributed" load acting away from the adherend end. All nodes of the adherend end were coupled in their first degree of freedom so that they move by the same amount in the 1-direction. These nodes were constrained against movement perpendicular to the load and against rotation around the 3-axis. The boundary conditions are illustrated in Figure 1. The basic single-lap joint specimen used in the analyses is shown in Figure 2 (see [30]). The same finite element mesh and boundary conditions were used in all cases. A non-linear solution algorithm was used.

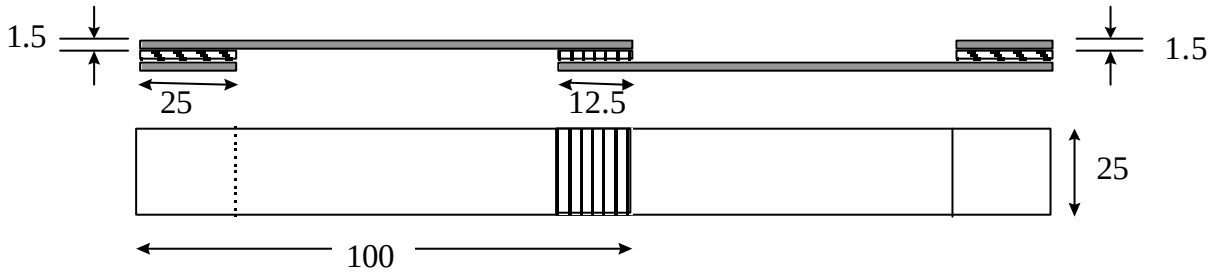

Figure 2: Single-lap joint test specimen.

The specimens were meshed to give the same geometry as actual test specimens (with the exception of the fillets at the ends of the joint). The ends of the joints were modelled as either having no fillet or having a fillet with a concave surface (Figure 3) with a radius equal in magnitude to the adhesive adhesive layer thickness. In practice, the fillets at the ends of joints were not precisely shaped. The finite element mesh was locally refined at the ends of the overlap.

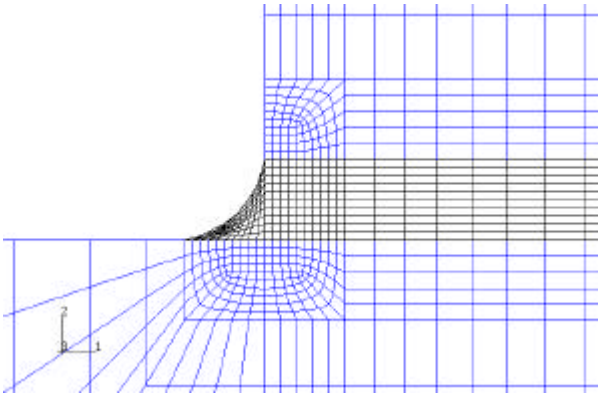

Figure 3: Concave fillet radius.

The large stress concentrations at the ends of the adhesive required the use of a non-linear material model. The von Mises and linear Drucker-Prager criterion were used to model deformation of the joint. Elastic property and stress/strain data for the adhesives were obtained from tensile and shear tests conducted on bulk adhesive specimens. Figure 4(a) shows a typical stress-strain response for AV119 (Araldite® 2007). The yield surface was defined by giving the value of the true uniaxial yield stress as a function of true uniaxial equivalent plastic strain. The mild steel adherend was also represented by the von Mises plasticity model using the stress-strain curves obtained from tensile tests on dumbbell specimens manufactured from the substrate material. Figure 4(b) shows a typical stress-strain response for CR1 mild steel (supplied by Corus).

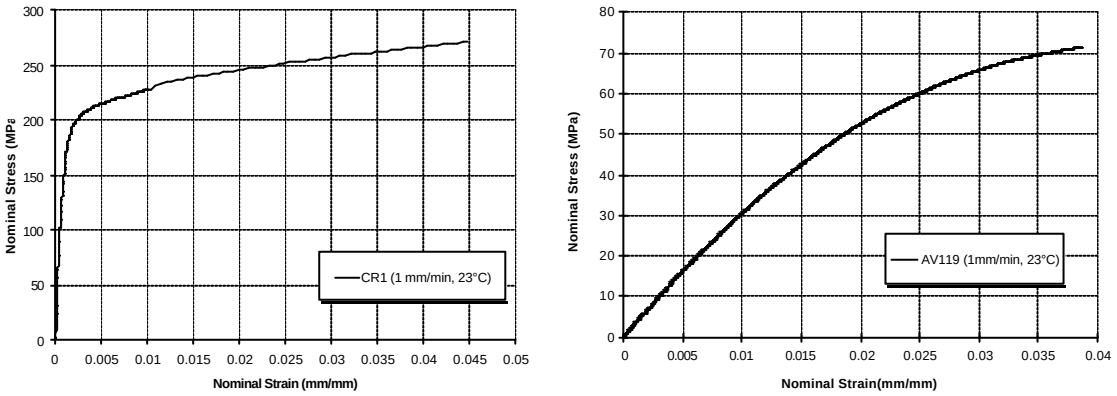

CR1 mild steel **AV119 epoxy adhesive**

Figure 4: Tension curves for calibration of elastic-plastic material model.

Typical tensile and shear properties for AV119 and XD4601 epoxy adhesives and the mild steel adherend are given in Tables 1 and 2.

Table 1: Typical Tensile and Shear Properties for AV119 and XD4601

Property	Adhesive	
	AV119	XD4601
Tension		
Modulus (GPa)	3.05	2.91
Strength (MPa)	71.3	57.6
Poisson's Ratio	0.34	0.37
Shear		
Modulus (GPa)	1.10	1.03
Strength (MPa)	41.0	42.3

Table 2: Typical Tensile and Shear Properties for CR1 Mild Steel (Average Value ± 1 Standard Deviation)

Property	Average
Tension	
Modulus (GPa)	206 ± 6
Poisson's Ratio	0.38 ± 0.02
Ultimate Strength (MPa)	334 ± 2
Yield Strength (MPa)	206 ± 1
Ultimate Strain (%)	4.23 ± 0.5
Yield Strain (%)	0.25 ± 0.01
Shear	
Modulus (GPa)	74 ± 4

The large difference in thickness between the adhesive and the adherend, and the large differences in mechanical properties of these materials leads to an ill-conditioned numerical problem. A series of FE models were analysed examining different mesh densities and element types in order to eliminate any numerical errors. The mesh was refined at the regions of high stress gradients by progressively increasing the element density, keeping their shape as close as possible to the original mesh.

FEA was used to investigate the effect of the following parameters on the joint strength:

- Adherend thickness (1.6, 2.4 and 3.2 mm)
- Adhesive thickness (0.25, 0.5, 1.0 and 2.0 mm)
- Bond (or overlap) length (12.5, 25.0 and 50.0 mm)
- Fillet geometry (square and concave)

3.2 SCARF JOINT

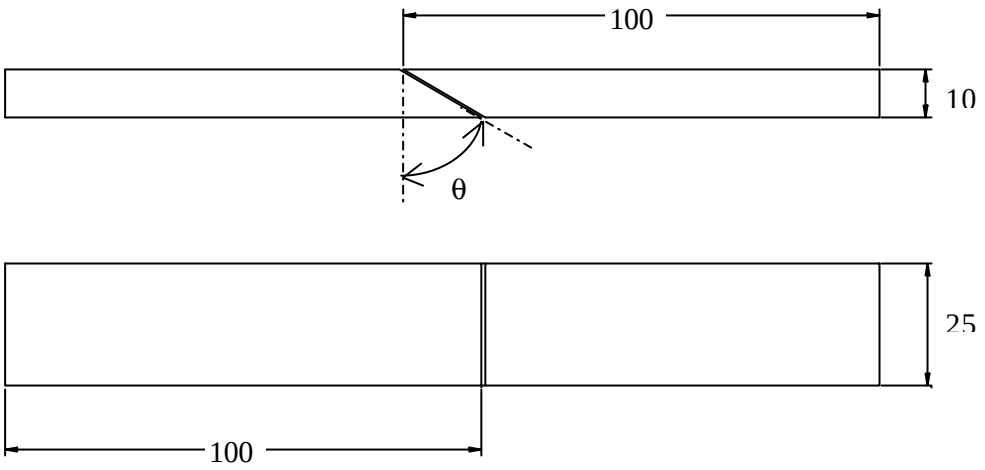

Figure 5: Schematic of scarf joint (mm).

A series of FEA simulations were conducted on the scarf joint in which the taper angle, q, and adhesive layer thickness were varied. The basic test geometry is shown in Figure 5. The boundary conditions were configured so that one end (end A) was fully constrained (i.e. no movement in the 1-, 2- or 3-direction) to simulate a fixed grip and the other end (end B) was restrained from rotating in the 2-direction. All the nodes at end B were tied to a single node (i.e. reference node), thus effectively preventing rotation and translation in the 2- and 3-directions. Displacements were applied in the 1-direction to the reference node to simulate extension of the scarf joint in the test machine and the total reaction force on the specimen is summed at the end node. This arrangement does not fully model the test machine as no allowance is made for the compliance of the test machine (particularly the out of plane compliance) or any imperfections in the test machine set-up (e.g. misalignment). Figure 6 shows the mesh used for FEA of the scarf joint.

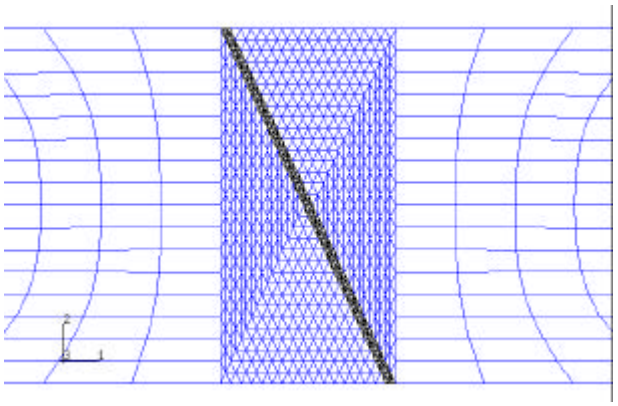

Figure 6: Finite element mesh diagram for scarf joint.

Uniaxial loading of the scarf joint results in a mixed shear / tensile stress state in the adhesive layer with the ratio of peel and shear stresses varying with the taper angle. As previously mentioned, FEA was used to investigate the effect of the following parameters on the joint strength:

- Taper angle (25°, 45° and 60°)

- Adhesive thickness (0.25, 0.5, 1.0 and 2.0 mm)

4. SINGLE-LAP JOINT ANALYSIS

This section presents the results of the numerical analyses conducted on CR1 mild steel single-lap joints bonded with AV119 to assess the reliability of different failure criteria (listed in Section 4.1) for predicting joint strength and assess the effects on the strength of key geometric parameters. A full factorial analysis has been carried out on the FEA data to determine empirical relationships between the main factors and joint strength. Predicted strength values are compared with experimental data and analytical predictions.

4.1 FAILURE CRITERIA

The following failure criteria have been assessed:

- Maximum tensile stress
- Maximum tensile strain
- Maximum shear stress
- Maximum shear strain
- Maximum principal strain
- Hill's failure criterion (Equation (13))

Hills's failure criterion or maximum work theory, developed for anisotropic materials (i.e. composites), is based on von Mises yield criterion for a homogeneous and isotropic solid. Assuming plane stress conditions, Hill's failure criterion can be written as:

$$\left(\frac{\sigma_{11}}{S_{11}}\right)^2+\left(\frac{\sigma_{22}}{S_{22}}\right)^2+\left(\frac{\tau_{12}}{S_{12}}\right)^2=1 \qquad (13)$$

where s_{11}, s_{22} and t_{12} are the in-plane longitudinal, transverse and shear stresses, and $\mathbf{S_{11}}$, $\mathbf{S_{22}}$ and $\mathbf{S_{12}}$ are the corresponding strengths in the principal material directions. In many cases, s_{33} will not be negligible. The failure criterion describes an ellipsoid failure criterion. For isotropic materials, $\mathbf{S_{11}}$ is equal to $\mathbf{S_{22}}$ and hence Equation (13) can be rewritten as follows:

$$\left(\frac{\sigma_{11}}{S_{11}}\right)^2+\left(\frac{\sigma_{22}}{S_{11}}\right)^2+\left(\frac{\tau_{12}}{S_{12}}\right)^2=1 \qquad (14)$$

The analytical analysis presented below neglects the lateral or transverse tensile stress component s_{22}. For the analytical analysis, Equation (14) reduces to the following:

$$\left(\frac{\sigma_{11}}{S_{11}}\right)^2+\left(\frac{\tau_{12}}{S_{12}}\right)^2=1 \qquad (15)$$

4.2 ANALYTICAL ANALYSIS

For a single-lap joint, the maximum adhesive shear stress, $\tau_{o,max}$, and peel stress, $\sigma_{o,max}$, can be calculated using the following equations [31]:

$$\tau_{o,max} = \frac{\sigma}{8}(1+3k)\sqrt{\frac{8G_a t}{E t_a}} \tag{16}$$

$$\frac{\sigma_{o,max}}{\sigma}\left(\frac{c}{t}\right)^2 = \lambda^2 \frac{k}{2}\frac{\sinh(2\lambda)-\sin(2\lambda)}{\sinh(2\lambda)+\sin(2\lambda)} - \lambda k' \frac{\cosh(2\lambda)+\cos(2\lambda)}{\sinh(2\lambda)+\sin(2\lambda)} \tag{17}$$

where:

$$\sigma = \frac{P}{t} \tag{18}$$

$$c = \frac{L}{2} \tag{19}$$

$$k = \frac{\cosh(u_2 c)\ \sinh(u_1 L)}{\sinh(u_1 L)\ \cosh(u_2 c) + 2\sqrt{2}\cosh(u_1 L)\sinh(u_2 c)} \tag{20}$$

$$u_1 = 2\sqrt{2}\, u_2 \tag{21}$$

$$u_2 = \sqrt{\frac{3\sigma(1-\nu^2)}{2Et^2}} \tag{22}$$

$$k' = k\, c\sqrt{\frac{3\sigma(1-\nu^2)}{E t^2}} \tag{23}$$

$$\lambda = \frac{c}{t}\left(\frac{6 E_a t}{E t_a}\right)^{1/4} \tag{24}$$

and

P = load per unit width
L = length of overlap (bond length)
t = adherend thickness
E = adherend modulus
$\mathbf{G_a}$ = adhesive shear modulus (initial)
$\mathbf{t_a}$ = adhesive layer thickness
$\mathbf{E_a}$ = adhesive tensile modulus
n = adherend Poisson's ratio

Failure loads for the single-lap joint were calculated using the above analytical solution in conjunction with the maximum shear stress and maximum tensile stress failure criteria, and the failure criterion described by Equation (15).

4.3 NUMERICAL RESULTS

A full factorial analysis was carried out on the FEA simulation results for the single-lap joints (FEA results are presented in Tables A1 to A4 in Appendix A). Table 3 shows the factors and levels used in the full matrix of tests (see Tables B1 and B2 in Appendix B for full test matrix for strength predictions based on von Mises and linear Drucker-Prager material models). The main factors (or parameters) **A**, **B** and **C** and their interactions (**A x B**, **A x C** and **B x C**) shown in Appendix B (Tables B3 and B4) correspond to adhesive thickness, adherend thickness and bond (or overlap) length, respectively.

Table 3: Factors and Levels for Full Matrix - Single-Lap Joint

Adhesive Thickness (mm)	Level	Adherend Thickness (mm)	Level	Bond Length (mm)	Level
0.25	1	1.6	1	12.5	1
0.50	2	2.4	2	25.0	2
1.00	3	3.2	3	50.0	3
2.00	4				

Tables 4 and 5 compare FEA simulation results with analytical predictions and experimental data. Five specimens were generally tested for each condition with interfacial failure occurring in all tests. The results presented in these tables are for joints with concave fillets (see Figure 3). A number of observations can be made in regard to the predictive analyses:

- Strength predictions for joints with fillets are invariably higher than those without a fillet as to be expected (see Tables A3 and A4 in Appendix A).
- The combination of Linear Drucker-Prager material model and maximum shear strain failure criteria provided the best estimate of joint strength.
- At short overlap lengths (i.e. 12.5 mm), the von Mises materials model is marginally more accurate than the Linear Drucker-Prager model.
- Strain based failure criteria are generally more accurate than the stress based failure criteria.
- Analytical approach seems to work best when combined with the maximum shear stress failure criteria (see Table 4), although this approach is far from satisfactory.

Table 4: Predicted Failure Loads (N) for CR1 Mild Steel/AV119 Single-Lap Joints Stress Based failure Criteria ($w = 25$ mm, $r = t_a = 0.25$ mm, $t = 2.5$ mm)

Stress Based Failure Criteria	Bond Length (mm)		
	12.5	25	50
Maximum Shear Stress (41.0 MPa)			
FEA - von Mises	6,285	7,655	10,482
FEA - Linear Drucker-Prager	6,110	7,540	12,287
Analytical solution	10,545	10,808	11,674
Maximum Tensile Stress (71.3 MPa)			
FEA - von Mises	6,295	7,715	10,656
FEA - Linear Drucker-Prager	6,105	7,517	12,175
Analytical solution	15,014	16,014	18,068
Hill's Failure Criterion			
FEA - von Mises (Eqn (14))	4,076	4,900	6,683
FEA - Linear Drucker-Prager (Eqn (14))	4,426	5,321	7,219
Analytical solution (Eqn 15))	8,627	8,968	9,818
Experimental	**8,850 ± 250**	**10,700 ± 950**	**15,825 ± 1,575**

Table 5: Predicted Failure Loads (N) for CR1 Mild Steel/AV119 Single-Lap Joints Strain Based failure Criteria ($w = 25$ mm, $r = t_a = 0.25$ mm, $t = 2.5$ mm)

Strain Based Failure Criteria	Bond Length (mm)		
	12.5	25	50
Maximum Shear Strain (0.2)			
FEA - Von Mises	8,711	10,168	13,512
FEA - Linear Drucker-Prager	7,985	10,594	13,930
Maximum Tensile Strain (0.04)			
FEA - Von Mises	7,395	9,526	12,833
FEA - Linear Drucker-Prager	7,280	9,282	12,727
Maximum Principal Strain (0.04)			
FEA - Von Mises	5,878	7,115	9,735
FEA - Linear Drucker-Prager	5,722	6,918	9,401
Experimental	**8,850 ± 250**	**10,700 ± 950**	**15,825 ± 1,575**

Statistical analysis (Qualitex-4, Nutek Inc. USA) was used to rank the relative importance of the main factors (i.e. adhesive thickness, adherend thickness and bond length) and their interactions on the strength of single-lap joints (see Table 6). It was clearly evident from the analysis that there were interactions between the three main factors, although this was difficult to express as an empirical formulation. The statistical analysis indicated that bond length was the predominant factor that determined the strength of the joint. In contrast, adherend thickness had a moderate effect on joint strength and adhesive thickness tended to have a minimal effect on the joint strength. The strongest interaction by a considerable margin was the interaction between the bond thickness and bond length (i.e. **A** x **C**). These observations and the rankings presented in Table 6 applied to all combinations of failure criterion and material models investigated in the study.

Table 6: Ranking of Main Factors and Interactions

Rank	Main Factors	Interactions
1	C	A x C
2	B	A X B
3	A	B X C

It was possible to relate the predicted joint strength to the two of the main factors (i.e. adherend thickness and bond length) using simple empirical relationships. The following formulations were derived for the combination of Linear Drucker-Prager materials model and the maximum shear strain failure criteria.

Adherend Thickness (t) Effect

$$P_{failure} = 3{,}878 + 3{,}085t \quad (25)$$

Bond length (L) Effect

$$P_{failure} = 5{,}999 + 131.5L \quad (26)$$

Adhesive Thickness (t_a) Effect

$$P_{failure} = 9{,}367 \pm 2{,}680 \quad (27)$$

The failure strength of the joint for any combination of the three main factors can be calculated from the three constitutive equations and the grand average performance (GAP) value obtained from the full factorial experiment. The equation for calculating the joint strength is given below:

$$\mathbf{P_{failure} = GAP + (Eqn\ (25) - GAP) + (Eqn\ (26) - GAP) + (Eqn\ (27) - GAP)} \quad (28)$$

Note: GAP value was calculated to be $9{,}637 \pm 2{,}680$ N.

The absolute difference between measured and predicted values decreases as the bond length increases. Table 7 shows a comparison between measured failure load and predictive model (Equation (28)) results.

Table 7: Predicted Failure Loads for CR1 Mild Steel/AV119 Single-Lap Joints Linear Drucker-Prager Materials Model and Maximum Shear Strain Failure Criteria ($w = 25$ mm, $r = t_{adhesive} = 0.25$ mm, $t_{adherend} = 2.5$ mm)

Bond Length (mm)	Failure Load (N)		
	Predicted	Measured	Difference (%)
12.5	9,867	$8{,}850 \pm 250$	11.49
25.0	11,510	$10{,}700 \pm 950$	7.57
50.0	14,768	$15{,}825 \pm 1{,}575$	-6.68

The question arises as to the applicability of using Equation (28) to predict the joint strength of test specimens with dimensions that were outside the FEA simulations. Tests were conducted on larger specimens (i.e. 50 mm wide with overlap lengths of 50 and 100 mm) and smaller specimens (i.e. 15 mm wide with overlap lengths of 12.5 mm). The specimens were

manufactured from 2.4 mm thick CR1 mild steel. The FEA results indicated that the failure load was directly proportional to the specimen width; independent of adhesive layer thickness, adherend thickness and bond length (i.e. increasing the width by a factor of 2 also increases the joint strength by a factor of 2).

The results presented in Table 8 show that the accuracy of the predictive model is less reliable for parameter values outside the full matrix of data used to derive Equation (28). The predictive values shown in Table 8 have been corrected to account for changes in specimen width. Table 8 also includes predicted strength values obtained from FEA runs carried out on the three joint configurations.

Table 8: Predicted Failure Loads (N) for CR1 Mild Steel/AV119 Single-Lap Joints Linear Drucker-Prager Materials Model and Maximum Shear Strain Failure Criteria ($r = t_{adhesive} = 0.25$ mm, $t_{adherend} = 2.5$ mm)

Specimen Width (mm)	Bond Length (mm)	Failure Load (N)		
		Predicted	Measured	Difference (%)
15.0	12.5	**Eqn(28):** 5,012 **FEA:** 4,940	4,610 ± 146	8.72
50.0	50	**Eqn(28):** 29,595 **FEA:** 26,430	31,940 ± 482	7.34
50.0	100	**Eqn(28):** 42,745 **FEA:** 29,622	36,737 ± 450	16.35

4.4 DISCUSSION

The analysis raised a number of issues, which will briefly be discussed in this section. The first issue relates to crack initiation. Figure 7 shows a single-lap joint in which failure has initiated at the adherend corners near the interface. The FEA in this study predicted that joints with concave fillets failed (i.e. plastic deformation and crack initiation) at the outer surface of the fillet with crack growth propagating at 45° across the fillet towards the adherend corners. It should be noted that cracking at the corners near the interface is predicted when the adhesive covers the end of the adherend and when there is no fillet present (see Figure 7). The stress concentrations are more or less independent of fillet shape and length for the configuration shown in Figure 7. The fillet geometry used in the analysis is a reasonable approximation of the fillets shown in Figure 7. Recent developments within PAJex1, to be published in a future NPL report, have led to improvements in FEA modelling of the joint in which the location of damage initiation and direction of damage propagation were accurately predicted.

FEA indicated in a number of cases that the steel adherends would plastically deform prior to adhesive failure. Plastic deformation of the adherends is known to increase the adhesive strains, thus contributing to joint failure. The FEA analysis for the joint configurations presented in Tables 4, 5 and 8 indicated that the adherend would yield at lower loads than those required to initiate adhesive failure. All the joints that were tested were permanently deformed. Although designers / engineers try to avoid plastic deformation in the adherends, it is unavoidable in single-lap joint geometries that comply with current national and international standards.

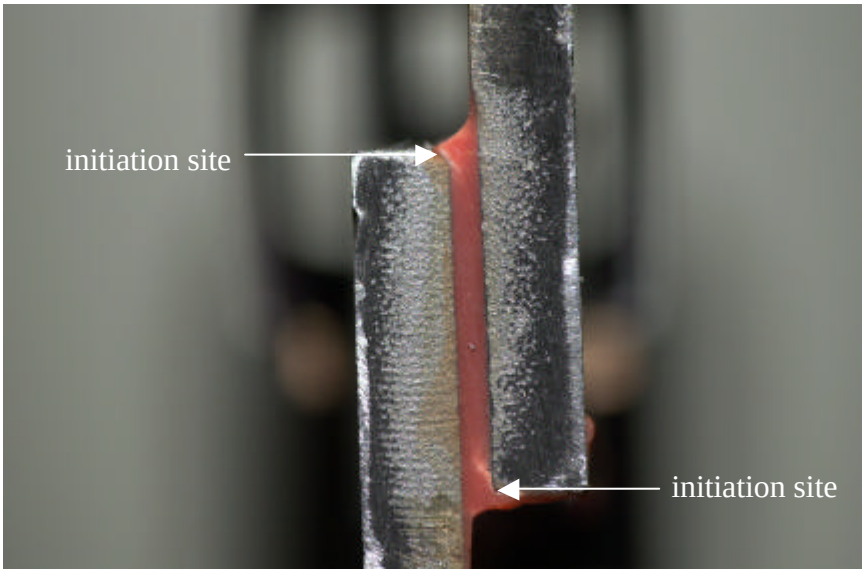

Figure 7: Failed single-lap joint.

Many of the materials model/failure criteria combinations indicated that there was an adhesive layer thickness effect, although the effect on joint strength was small in comparison with the effects of adherend thickness and bond length. The FEA results indicated that joint strength increases with adhesive layer thickness reaching a maximum value at 1 mm. The joint strength was expected to decrease when the adhesive layer thickness exceeded 1 mm. This trend was not observed for the combination of Linear Drucker-Prager/maximum shear strain failure criteria.

5. SCARF JOINT ANALYSIS

FEA simulations were conducted on mild steel scarf joints bonded with XD4601 and AV119 epoxy adhesives in order to assess the reliability of different failure criteria (listed in Section 4.1) for predicting joint strength. The FEA results were used to assess the effects of taper angle (i.e. 25°, 45° and 60°) and adhesive layer thickness (i.e. 0.25, 0.5 and 1.0 mm) on the joint strength. A full factorial analysis has been carried out on the FEA data from simulations carried out on the scarf joints bonded with XD4601 to determine empirical relationships between the main factors and joint strength. Predicted strength values are compared with experimental data and analytical predictions.

5.1 ANALYTICAL ANALYSIS

A simple strength-of-materials analysis approach [31], resolving stresses and areas, can be used to determine shear stress τ and normal stress σ_T in a simple scarf joint. The analysis predicts a uniform shear stress in the adhesive layer given by [31]:

$$\tau = P \sin\theta \cos\theta / t \tag{29}$$

and a uniform normal stress in the adhesive given by:

$$\sigma_T = P \cos^2\theta / t \tag{30}$$

where **P** is the applied (end) load per unit width, **t** is the adherend thickness and q is the taper angle.

The ratio of normal stress to shear stress is given by:

$$\sigma_T / \tau = \cot\theta \tag{31}$$

For a taper angle q = 60°, s_T/t is equal to 0.57. From a designer's perspective, the taper angle should be as large as possible. For repair applications, q is required to be greater than 87° (i.e. s_T/t = 0.05).

In principle, the load bearing capacity increases in proportion with the thickness of the adherends and is not limited by local stress concentrations at the overlap ends. The above analysis assumes that as the shear stress distribution is uniform and that there is no elastic trough in the stress distribution along the adhesive layer to alleviate continuous strains (deformations) under prolonged loading (e.g. creep or low frequency cyclic fatigue loads). FEA was carried out to verify if these assumptions were valid (see Section 5.2) and to determine the effect of varying taper angle and adhesive layer thickness on joint strength.

5.2 NUMERICAL RESULTS

A full factorial analysis was carried out on the FEA simulation results for the scarf joints (FEA results are presented in Tables C1 to C4 in Appendix C). The joints were 25 mm wide and 10 mm thick. Table 9 shows the factors and levels used in the full matrix of tests (see Tables D1 and D2 in Appendix D for full test matrix for strength predictions based on von Mises and linear Drucker-Prager material models). The main factors (or parameters) **A** and **B** and their interaction (**A x B**) shown in Appendix D (Tables D3 to D6) correspond to taper angle and adhesive layer thickness, respectively.

Table 9: Factors and Levels for Full Matrix - Scarf Joint

Taper Angle (degrees)	Level	Adhesive Thickness (mm	Level
25	1	0.25	1
45	2	0.50	2
60	3	1.00	3

Tables 10 to 13 compare FEA simulation results (stress and strain based failure criteria) with analytical predictions and experimental data. The FEA results have been corrected to allow for the fact that the test specimens were only 15 mm wide. It should be noted that the problem of convergence prevented a number of FEA runs to be completed.

Table 10: Predicted Failure Loads (N) for Mild Steel/AV119 Scarf Joints Stress Based failure Criteria (w = 15 mm, $t_{adhesive}$ = 0.25 mm, $t_{adherend}$ = 10 mm)

Stress Based Failure Criteria	Taper Angle (degrees)		
	25	45	60
Maximum Shear Stress (41.0 MPa)			
FEA - von Mises	15,320	12,264	13,663
FEA - Linear Drucker-Prager	-	11,629	13,327
Analytical solution	16,057	12,300	14,203
Maximum Tensile Stress (71.3 MPa)			
FEA - von Mises	15,406	12,340	14,056
FEA - Linear Drucker-Prager	-	11,606	13,286
Analytical solution	13,020	21,390	42,780
Hill's Failure Criterion			
FEA - von Mises (Eqn (14))	8,851	10,479	12,761
FEA - Linear Drucker-Prager (Eqn (14))	9,234	11,069	14,020
Analytical solution (Eqn (15))	10,113	10,663	13,479
Experimental	**10,053** ± **133**	**12,806** ± **384**	**15,870** ± **278**

Table 11: Predicted Failure Loads (N) for Mild Steel/AV119 Scarf Joints Strain Based failure Criteria (w = 15 mm, $t_{adhesive}$ = 0.25 mm, $t_{adherend}$ = 10 mm)

Strain Based Failure Criteria	Taper Angle (degrees)		
	25	45	60
Maximum Shear Strain (0.2)			
FEA - Von Mises	15,461	-	-
FEA - Linear Drucker-Prager	11,687	-	12,286
Maximum Tensile Strain (0.04)			
FEA - Von Mises	11,731	10,164	13,936
FEA - Linear Drucker-Prager	10,434	10,820	13,283
Maximum Principal Strain (0.04)			
FEA - Von Mises	11,095	10,162	13,890
FEA - Linear Drucker-Prager	10,399	10,810	14,788
Experimental	**10,053** ± **133**	**12,806** ± **384**	**15,870** ± **278**

Table 12: Predicted Failure Loads (N) for Mild Steel/XD4601 Scarf Joints Stress Based failure Criteria (w = 15 mm, $t_{adhesive}$ = 0.25 mm, $t_{adherend}$ = 10 mm)

Stress Based Failure Criteria	Taper Angle (degrees)		
	25	45	60
Maximum Shear Stress (42.3 MPa)			
FEA - von Mises	14,822	12,258	13,352
FEA - Linear Drucker-Prager	-	11,578	13,574
Analytical solution	16,567	12,690	14,653
Maximum Tensile Stress (57.6 MPa)			
FEA - von Mises	13,680	9,671	10,760
FEA - Linear Drucker-Prager	9,655	9,364	10,586
Analytical solution	10,519	17,280	34,560
Hill's Failure Criterion			
FEA - von Mises (Eqn (14))	7,415	8,513	10,495
FEA - Linear Drucker-Prager (Eqn (14))	7,528	8,803	12,319
Analytical solution (Eqn (15))	8,880	10,228	13,491
Experimental	**7,618** ± **237**	**10,470** ± **254**	**13,240** ± **191**

Table 13: Predicted Failure Loads (N) for Mild Steel/XD4601 Scarf Joints Strain Based failure Criteria (w = 15 mm, $t_{adhesive}$ = 0.25 mm, $t_{adherend}$ = 10 mm)

Strain Based Failure Criteria	Taper Angle (degrees)		
	25	45	60
Maximum Shear Strain (0.145)			
FEA - Von Mises	12,153	12,577	22,065
FEA - Linear Drucker-Prager	9,768	-	13,073
Maximum Tensile Strain (0.074)			
FEA - Von Mises	11,416	9,920	11,292
FEA - Linear Drucker-Prager	8,585	15,292	12,376
Maximum Principal Strain (0.074)			
FEA - Von Mises	11,020	9,919	11,195
FEA - Linear Drucker-Prager	8,416	9,162	11,668
Experimental	**7,618** ± **237**	**10,470** ± **254**	**13,240** ± **191**

A number of observations can be made in regard to the predictive analyses:

- Linear Drucker-Prager material model combined with maximum principal strain failure criteria generally provided the best estimate of joint strength.
- Strength calculations based on the Linear Drucker-Prager materials model are generally more accurate than strength values for the von Mises materials model.
- Strain based failure criteria are generally more accurate than the stress based failure criteria.
- Calculated strength values based on the analytical approach combined with the Hill's failure criteria (see Tables 10 and 12) are in reasonable agreement with experimental data for the two adhesive systems.

It was possible to estimate the failure load of mild steel/XD4601 scarf joints using simple empirical relationships. The following formulations were derived for the analytical approach using Hill's (stress based) failure criteria (see Equation (15)) and the Linear Drucker-Prager materials model combined with the maximum shear strain failure criteria.

5.2.1 Linear Drucker-Prager Materials Model / Maximum Principal Strain Failure Criteria

Taper Angle (q) Effect

$$P_{failure} = 13{,}931 + 412.6e^{(\theta - 31.78)/11.04} \quad (32)$$

Adhesive Thickness (t_a) Effect

$$P_{failure} = 18{,}914 \pm 2{,}691 \quad (33)$$

The failure strength of the joint for any combination of the two main factors can be calculated from the two constitutive equations and the grand average performance (GAP) value obtained from the full factorial experiment. The equation for calculating the joint strength is given below:

$$\mathbf{P_{failure} = GAP + (Eqn\ (32) - GAP) + (Eqn\ (33) - GAP)} \quad (34)$$

Note: GAP value was calculated to be $18{,}914 \pm 2{,}691$ N.

The absolute difference between measured and predicted values remains constant with taper angle (i.e. bond length). According to the FEA, adhesive layer thickness has no apparent effect on the joint strength. Table 14 compares measured and predicted (Equation (34)) strength values. Predicted results have been corrected to allow for the fact that the test specimens were only 15 mm wide. The butt-tension strength (i.e. $\theta = 0°$) is predicted to be 55.8 MPa, which is almost the same as the tensile strength of the adhesive (57.6 MPa).

Table 14: Predicted Failure Loads for Mild Steel/XD4601 Scarf Joints Linear Drucker-Prager Materials Model and Maximum Principal Strain Failure Criteria

Taper Angle (degrees)	Failure Load (N)		
	Predicted	Measured	Difference (%)
25	8,582	$7{,}618 \pm 237$	12.65
45	9,178	$10{,}470 \pm 254$	-12.34
60	11,555	$13{,}240 \pm 191$	-12.73

5.2.2 Analytical Solution / Hill's (Stress Based) Failure Criteria

The relationship between failure load and taper angle can be represented by exponential growth functions as shown in Equations (35) and (36).

Taper Angle (q) Effect - Mild Steel/AV119 Scarf Joint

$$P_{failure} = 10{,}051 + 143.9e^{(\theta - 32.41)/8.70} \quad (35)$$

Taper Angle (q) Effect - Mild Steel/XD4601 Scarf Joint

$$P_{failure} = 8{,}425 + 657.6e^{(\theta - 30.36)/14.52} \quad (36)$$

The above relationships predict that the butt tension failure load (i.e. $\theta = 0°$) for AV119 and XD4601 is 10,054 N (67.0 MPa) and 8,505 N (56.7 MPa), respectively. These values are in

good agreement with tensile strength values of 71.3 MPa and 57.6 MPa measured for the two adhesives.

6. DISCUSSION AND CONCLUDING REMARKS

The results presented in this report show that for the two joint configurations bonded with epoxy adhesives AV119 and XD4601 simple algebraic relationships can be used to estimate the effects of the geometric parameters on joint strength. The equations however are empirical, and therefore not related to any physical mechanism. The overall equations relating the main factors are only as good as the constitutive relationships incorporated. Any deficiencies in these relationships will result in poor correlation between predictive model and the measured data. In addition, the uncertainty can be expected to increase for specimen geometries outside the test matrix.

The results from the evaluation of the factorial test show that the key parameter for the single-lap joint was bond length as to be expected. In contrast, adherend thickness had a moderate effect on joint strength and adhesive thickness tended to have a minimal effect on the joint strength. The strongest interaction by a considerable margin was the interaction between the bond thickness and bond length. In the case of the scarf joint, taper angle was the controlling factor and adhesive layer thickness had only a marginal effect on joint strength. In both cases the joint strength was linearly proportional to the specimen width.

It was not possible to identify one single combination of materials model and failure criteria that could be applied to the two joint configurations and two adhesive systems studied in this programme. The results indicated:

Single-Lap Joints: Linear Drucker-Prager material model combined with maximum shear strain failure criteria generally provided the best estimate of joint strength.

Scarf Joints: Linear Drucker-Prager material model combined with maximum principal strain failure criteria generally provided the best estimate of joint strength.

Additional Comments

- Strength calculations based on the Linear Drucker-Prager materials model are generally more accurate than strength values for the von Mises materials model.
- Strain based failure criteria are generally more accurate than the stress based failure criteria

In summary, there is still a need for a robust failure criterion that can be universally applied to all bonded structures. Analytical formulations have a limited value, although in the case of the scarf joint it was possible to use Hill's failure criterion to predict joint strength with reasonable accuracy.

ACKNOWLEDGEMENTS

This work forms part of the extension programme for "Performance of Adhesive Joints" funded by the Engineering Industries Directorate of the UK Department of Trade and Industry, as part of its support of the technological competitiveness of UK industry. The authors would like to express their gratitude to all members of the Industrial Advisory Group (IAG) and to colleagues at the National Physical Laboratory, particularly to Mr G Hinopoulos, Dr G Dean, Mr B Duncan, Ms E Arranz Mr R Mera and Mr A Pearce whose contributions and advice have made the work possible.

REFERENCES

1. Broughton, W.R. and Hinopoulos, G., "Evaluation of the Single-Lap Joint Using Finite Element Analysis", NPL Report CMMT(A)206, 1999.
2. Hinopoulos, G. and Broughton, W.R., "Evaluation of the T-Peel Joint Using the Finite Element Method", NPL Report CMMT(A)207, 1999.
3. Hart-Smith, L.J., "Adhesive-Bonded Single-Lap Joints", NASA Report CR-112236, 1973.
4. Hart-Smith, L.J., "Adhesive-Bonded Scarf and Stepped-Lap Joints", NASA Report CR-112237, 1973.
5. Hart-Smith, L.J., "Adhesive-Bonded Double-Lap Joints", NASA Report CR-112238, 1973.
6. Hart-Smith, L.J., "Analysis and Design of Advanced Composite Bonded Joints", NASA Report CR-2218, 1974.
7. Harris, J.A. and Adams, R.D., "Strength Prediction of Bonded Single Lap Joints by Non-Linear Finite Element Methods", International Journal of Adhesion and Adhesives, Volume 4, Number 2, 1984, pp 65-78.
8. Adams, R.D., "The Mechanics of Bonded Joints, Structural Adhesives in Engineering, ImechE Conference Publications, Suffolk, 1986, pp 17-24.
9. "Adhesives and Sealants", Engineered Materials Handbook, Volume 3, ASM International, 1990.
10. "Composites Engineering Handbook", Edited by Mallick, P.K., Marcel Dekker, Inc., 1997.
11. "Mechanical Properties of Solid Polymers", Ward, I.M., John Wiley & Sons, Ltd, 1971.
12. Bowden, P.B. and Dukes, J.A., "The Plastic Flow of Isotropic Polymers", Journal of Materials Science, Volume 7, 1972, pp 52-63.
13. "Introduction to Polymers", Young, R.J., Chapman and Hall, 1981.
14. Wang, C.H. and Chalkley., "Plastic Yielding of A Film Adhesive Under Multiaxial Stresses", International Journal of Adhesion and Adhesives, Volume 20, Number 2, 2000, pp 155-164.
15. Dean, G.D. and Crocker, L., "Comparison of the Measured and Predicted Deformation of an Adhesively Bonded Lap-Joint Specimen", NPL Report CMMT(A)293, 2000.
16. Read, B.E., Dean, G.D. and Ferriss, D.H., "An Elastic-Plastic Model for the Non-Linear Mechanical Behaviour of Rubber-Toughened Adhesives", NPL Report CMMT(A)289, 2000.
17. Gurson, A.L., "Continuum Theory of Ductile Rupture by Void Nucleation and Growth: Part 1 – Yield Criteria and Flow Rules for Porous Ductile Meadia", Journal of Engineering Materials Technology, Transactions of ASME, Volume 99, 1977, pp 2-15.
18. "Physics of Glassy Polymers", Second Edition, Edited by Haward, R.N. and Young, R.J., Chapman and Hall, London, 1997.

19. Lazzeri, A. and Bucknall, C.B., "Dilatational Bands in Rubber-Toughened Polymers", Journal of Materials Science, Volume 28, 1993, pp 6799-6808.
20. Groth, H.L., "A Method to Predict Fracture in an Adhesively Bonded Joint", International Journal of Adhesion and Adhesives, Volume 5, Number 1, 1985, pp 19-22.
21. Groth, H.L., "Stress Singularities and Fracture at Interface Corners in Bonded", International Journal of Adhesion and Adhesives, Volume 8, Number 2, 1999, pp 107-113.
22. Fernlund, G. and Spelt, J.K., "Failure Load Prediction: I. Analytical Method", International Journal of Adhesion and Adhesives, Volume 11, Number 4, 1991, pp 213-220.
23. Fernlund, G. and Spelt, J.K., "Failure Load Prediction: II. Experimental Results", International Journal of Adhesion and Adhesives, Volume 11, Number 4, 1991, pp 221-227.
24. Fernlund, G., Papini, M., McCammond, D. and Spelt, J.K., "Fracture Load Predictions for Adhesive Joints", Composites Science and Technology, Volume 51, 1994, pp 587-600.
25. Ashcroft, I.A, Gilmore, R.B and Shaw, S.J., "Cyclic Fatigue and Environmental Effects with Adhesively Bonded Joints", AGARD 83rd SMP Meeting, Florence, 1996.
26. Curley, A.J., Hadavinia, H., Kinloch, A.J. and Taylor, A.C., "Predicting the Service-Life of Adhesively-Bonded Joints", International Journal of Fracture, Volume 103, 2000, pp 41-69.
27. Towse, A., Potter, K.D., Wisnom, M.R. and Adams, R.D., "The Sensitivity of a Weibull Failure Criterion to Singularity Strength and Local Geometry Variations", International Journal of Adhesion and Adhesives, 19, 1999, pp 71-82.
28. "ABAQUS User's Manual", Version 5.8, HKS Inc., USA, 1998.
29. "FEMGV User's Manual", Version 5.1, FEMSYS Ltd., 1998.
30. BS EN 1465:1995, "Adhesives - Determination of Tensile Lap-shear Strength of Rigid-to-Rigid Bonded Assemblies".
31. "Structural Design of Polymer Composites", EUROCOMP Design Code and Handbook, Clarke, J.L., Editor, E and F.N. Spon, 1996.

APPENDICES

Table A1: FEA Strength Predictions for CR1 Mild Steel/AV119 Epoxy Single-Lap Joints (von Mises material model)

Case	Adhesive Thickness (mm)	Adherend Thickness (mm)	Bond Length (mm)	Predicted Failure Load (N)					
				Maximum Shear Stress	Maximum Tensile Stress	Hill's Failure Criterion	Maximum Shear Strain	Maximum Tensile Strain	Maximum Principal Strain
1	0.25	1.6	12.5	4,691	4,752	3,220	-	5,369	4,416
2	0.25	2.4	12.5	6,180	6,230	4,004	7,530	7,172	5,750
3	0.25	3.2	12.5	7,300	7,394	4,560	8,987	8,753	6,870
4	0.50	1.6	12.5	5,150	5,176	3,604	6,494	5,323	4,584
5	0.50	2.4	12.5	7,022	7,189	4,695	8,117	7,235	6,304
6	0.50	3.2	12.5	8,175	9,173	5,455	9,797	9,056	7,679
7	1.00	1.6	12.5	4,129	4,140	3,518	5,213	4,273	3,900
8	1.00	2.4	12.5	6,094	6,114	4,881	7,401	6,214	5,843
9	1.00	3.2	12.5	8,149	8,507	6,141	9,796	8,556	7,959
10	2.00	1.6	12.5	4,317	4,927	3,237	9,294	4,175	3,968
11	2.00	2.4	12.5	6,313	6,688	4,901	9,738	6,201	5,858
12	2.00	3.2	12.5	8,173	9,172	6,256	-	8,257	7,800
13	0.25	1.6	25.0	6,298	6,362	3,978	8,752	7,555	5,718
14	0.25	2.4	25.0	7,504	7,621	4,823	9,982	9,242	6,960
15	0.25	3.2	25.0	8,830	8,945	5,515	11,143	10,780	8,178
16	0.50	1.6	25.0	7,193	7,411	4,580	9,162	7,733	6,358
17	0.50	2.4	25.0	8,931	9,164	5,751	11,043	9,840	7,881
18	0.50	3.2	25.0	10,210	11,010	6,778	-	11,218	9,373
19	1.00	1.6	25.0	6,312	6,412	4,583	9,259	7,486	6,304
20	1.00	2.4	25.0	8,728	8,873	6,453	11,572	9,319	8,088
21	1.00	3.2	25.0	10,565	10,839	7,752	13,369	10,983	9,943
22	2.00	1.6	25.0	-	-	-	-	-	-
23	2.00	2.4	25.0	-	-	-	-	-	-
24	2.00	3.2	25.0	-	-	-	-	-	-
25	0.25	1.6	50.0	8,655	8,702	5,593	9,772	8,884	7,994
26	0.25	2.4	50.0	10,595	10,761	6,552	13,137	12,420	9,941
27	0.25	3.2	50.0	11,603	11,758	7,386	14,972	14,662	10,768
28	0.50	1.6	50.0	9,445	9,617	6,597	9,860	9,040	8,523
29	0.50	2.4	50.0	12,088	12,254	7,859	13,909	12,687	10,925
30	0.50	3.2	50.0	13,876	14,355	8,999	-	15,226	12,487
31	1.00	1.6	50.0	9,452	9,543	7,412	9,942	9,269	8,725
32	1.00	2.4	50.0	12,021	12,287	9,231	14,151	13,095	11,725
33	1.00	3.2	50.0	14,234	14,280	10,764	17,912	15,356	13,793
34	2.00	1.6	50.0	-	-	-	-	-	-
35	2.00	2.4	50.0	-	-	-	-	-	-
36	2.00	3.2	50.0	-	-	-	-	-	-

Table A2: FEA Strength Predictions for CR1 Mild Steel/AV119 Epoxy Single-Lap Joints (Linear Drucker-Prager material model)

Case	Adhesive Thickness (mm)	Adherend Thickness (mm)	Bond Length (mm)	Predicted Failure Load (N)					
				Maximum Shear Stress	Maximum Tensile Stress	Hill's Failure Criterion	Maximum Shear Strain	Maximum Tensile Strain	Maximum Principal Strain
1	0.25	1.6	12.5	4,703	4,678	3,455	6,340	5,335	4,305
2	0.25	2.4	12.5	6,005	5,993	3,542	7,789	7,062	5,646
3	0.25	3.2	12.5	7,087	7,060	4,968	-	-	6,645
4	0.50	1.6	12.5	5,385	5,291	3,817	7,330	5,240	4,585
5	0.50	2.4	12.5	7,445	7,322	4,998	-	7,179	6,203
6	0.50	3.2	12.5	9,452	9,312	5,886	-	9,007	7,523
7	1.00	1.6	12.5	4,022	4,012	3,778	6,874	4,511	4,149
8	1.00	2.4	12.5	5,915	5,899	5,198	8,414	6,288	5,967
9	1.00	3.2	12.5	8,322	8,261	6,491	-	8,630	7,971
10	2.00	1.6	12.5	-	-	-	-	-	-
11	2.00	2.4	12.5	-	-	-	-	-	-
12	2.00	3.2	12.5	-	-	-	-	-	-
13	0.25	1.6	25.0	6,891	6,852	4,278	9,004	7,522	5,556
14	0.25	2.4	25.0	7,454	7,429	5,195	-	9,077	6,778
15	0.25	3.2	25.0	8,448	8,439	5,991	-	-	7,932
16	0.50	1.6	25.0	7,730	7,550	4,902	9,889	7,607	6,295
17	0.50	2.4	25.0	9,749	9,517	6,170	-	9,318	7,731
18	0.50	3.2	25.0	11,589	11,338	7,262	-	11,099	9,123
19	1.00	1.6	25.0	6,598	6,532	5,386	10,290	7,740	6,523
20	1.00	2.4	25.0	8,422	8,360	6,867	-	9,458	8,220
21	1.00	3.2	25.0	10,387	10,285	8,246	-	11,095	9,957
22	2.00	1.6	25.0	-	-	-	-	-	-
23	2.00	2.4	25.0	-	-	-	-	-	-
24	2.00	3.2	25.0	-	-	-	-	-	-
25	0.25	1.6	50.0	8,764	8,735	6,040	10,082	8,949	7,841
26	0.25	2.4	50.0	13,184	12,278	7,090	13,605	12,332	9,226
27	0.25	3.2	50.0	11,963	11,944	8,003	-	14,360	10,522
28	0.50	1.6	50.0	8,932	8,895	7,111	-	9,053	8,607
29	0.50	2.4	50.0	12,628	12,423	8,367	-	13,841	10,735
30	0.50	3.2	50.0	15,258	15,065	9,636	-	15,010	12,187
31	1.00	1.6	50.0	8,938	8,919	8,095	10,704	9,416	8,954
32	1.00	2.4	50.0	12,130	12,046	9,954	15,321	13,114	11,926
33	1.00	3.2	50.0	14,526	14,399	11,505	-	15,573	13,989
34	2.00	1.6	50.0	-	-	-	-	-	-
35	2.00	2.4	50.0	-	-	-	-	-	-
36	2.00	3.2	50.0	-	-	-	-	-	-

Table A3: FEA Strength Predictions for CR1 Mild Steel/AV119 Epoxy Single-Lap Joints - von Mises Material Model (concave fillet versus no fillet)

Case	Adhesive Thickness (mm)	Adherend Thickness (mm)	Bond Length (mm)	Predicted Failure Load (N)					
				Maximum Shear Stress	Maximum Tensile Stress	Hill's Failure Criterion	Maximum Shear Strain	Maximum Tensile Strain	Maximum Principal Strain
1 (no fillet)	0.25	2.5	12.5	4,225	4,240	2,241	6,043	7,507	3,904
2 (no fillet)	0.25	2.5	25.0	5,077	5,088	2,688	6,672	9,773	4,693
3 (no fillet)	0.25	2.5	50.0	6,577	6,525	3,743	10,076	13,217	6,497
4 (fillet)	0.25	2.5	12.5	6,285	6,295	4,076	8,711	7,395	5,878
5 (fillet)	0.25	2.5	25.0	7,655	7,715	4,900	10,168	9,526	7,115
6 (fillet)	0.25	2.5	50.0	10,482	10,656	6,683	13,512	12,833	9,735

Table A4: FEA Strength Predictions for CR1 Mild Steel/AV119 Epoxy Single-Lap Joints – Linear Drucker-Prager Material Model (concave fillet versus no fillet)

Case	Adhesive Thickness (mm)	Adherend Thickness (mm)	Bond Length (mm)	Predicted Failure Load (N)					
				Maximum Shear Stress	Maximum Tensile Stress	Hill's Failure Criterion	Maximum Shear Strain	Maximum Tensile Strain	Maximum Principal Strain
1 (no fillet)	0.25	2.5	12.5	5,330	5,264	2,659	-	-	-
2 (no fillet)	0.25	2.5	25.0	6,401	6,328	3,217	7,406	9,394	4,395
3 (no fillet)	0.25	2.5	50.0	8,777	8,666	4,498	10,164	13,027	5,679
4 (fillet)	0.25	2.5	12.5	6,110	6,105	4,426	7,985	7,280	5,722
5 (fillet)	0.25	2.5	25.0	7,540	7,517	5,321	10,594	9,282	6,918
6 (fillet)	0.25	2.5	50.0	12,287	12,175	7,219	13,930	12,727	9,401

Table B1: Full Matrix of FEA Simulations for Strength Predictions for CR1 Mild Steel/AV119 Epoxy Single-Lap Joints (von Mises material model)

Run	Main Factors			Interactions			Predicted Failure Load (N)					
	A	B	C	A x B	A x C	B x C	Maximum Shear Stress	Maximum Tensile Stress	Hill's Failure Criterion	Maximum Shear Strain	Maximum Tensile Strain	Maximum Principal Strain
1	1	1	1	1	1	1	4,691	4,752	3,220	-	5,369	4,416
2	1	1	2	1	2	2	6,298	6,362	3,978	8,752	7,555	5,718
3	1	1	3	1	3	3	8,655	8,702	5,593	9,772	8,884	7,994
4	1	2	1	2	1	2	6,180	6,230	4,004	7,530	7,172	5,750
5	1	2	2	2	2	2	7,504	7,621	4,823	9,982	9,242	6,960
6	1	2	3	2	3	3	10,595	10,761	6,652	13,137	12,420	9,941
7	1	3	1	3	1	3	7,300	7,394	4,560	8,987	8,753	6,870
8	1	3	2	3	2	3	8,830	8,945	5,515	11,143	10,780	8,178
9	1	3	3	3	3	3	11,603	11,758	7,386	14,972	14,662	10,768
10	2	1	1	2	2	1	5,150	5,176	3,604	6,494	5,323	4,584
11	2	1	2	2	2	2	7,193	7,411	4,580	9,162	7,733	6,358
12	2	1	3	2	3	3	9,445	9,617	6,597	9,860	9,040	8,523
13	2	2	1	2	2	2	7,022	7,189	4,695	8,117	7,235	6,304
14	2	2	2	2	2	2	8,931	9,164	5,751	11,043	9,480	7,881
15	2	2	3	2	2	3	12,088	12,254	7,859	13,909	12,687	10,925
16	2	3	1	3	2	2	8,175	9,173	5,455	9,797	9,056	7,679
17	2	3	2	3	3	2	10,210	11,010	6,778	-	11,218	9,373
18	2	3	3	3	3	3	13,876	14,355	8,999	-	15,226	12,487
19	3	1	1	3	3	1	4,129	4,140	3,518	5,213	4,273	3,900
20	3	1	2	3	3	3	6,312	6,412	4,583	9,259	7,486	6,304
21	3	1	3	3	3	3	9,452	9,543	7,412	9,942	9,269	8,725
22	3	2	1	3	3	2	6,094	6,114	4,881	7,401	6,214	5,843
23	3	2	2	3	3	3	8,728	8,873	6,453	11,572	9,319	8,088
24	3	2	3	3	3	3	12,021	12,287	9,231	14,151	13,095	11,725
25	3	3	1	3	3	3	8,149	8,507	6,141	9,796	8,556	7,959
26	3	3	2	3	3	3	10,565	10,839	7,752	13,369	10,983	9,943
27	3	3	3	3	3	3	14,234	14,280	10,764	17,912	15,356	13,793
28	4	1	1	4	4	1	4,317	4,927	3,237	9,294	4,175	3,968
29	4	1	2	4	4	2	-	-	-	-	-	-
30	4	1	3	4	4	3	-	-	-	-	-	-
31	4	2	1	4	4	2	6,313	6,688	4,901	9,738	6,201	5,858
32	4	2	2	4	4	2	-	-	-	-	-	-
33	4	2	3	4	4	3	-	-	-	-	-	-
34	4	3	1	4	4	3	8,173	9,172	6,256	-	8,257	7,800
35	4	3	2	4	4	3	-	-	-	-	-	-
36	4	3	3	4	4	3	-	-	-	-	-	-

A denotes adhesive layer thickness, B denotes adherend thickness and C denotes bond length.

Table B2: Full Matrix of FEA Simulations for Strength Predictions for CR1 Mild Steel/AV119 Epoxy Single-Lap Joints (Linear Drucker-Prager material model)

Run	Main Factors			Interactions			Predicted Failure Load (N)					
	A	B	C	A x B	A x C	B x C	Maximum Shear Stress	Maximum Tensile Stress	Hill's Failure Criterion	Maximum Shear Strain	Maximum Tensile Strain	Maximum Principal Strain
1	1	1	1	1	1	1	4,703	4,678	3,455	6,340	5,335	4,305
2	1	1	2	1	2	2	6,891	6,852	4,278	9,004	7,522	5,556
3	1	1	3	1	3	3	8,764	8,735	6,040	10,082	8,949	7,841
4	1	2	1	2	1	2	6,005	5,993	3,542	7,789	7,062	5,646
5	1	2	2	2	2	2	7,454	7,429	5,195	-	9,077	6,778
6	1	2	3	2	3	3	13,184	12,278	7,090	13,605	12,332	9,226
7	1	3	1	3	1	3	7,087	7,060	4,968	-	-	6,645
8	1	3	2	3	2	3	8,448	8,439	5,991	-	-	7,932
9	1	3	3	3	3	3	11,963	11,944	8,003	-	14,360	10,522
10	2	1	1	2	2	1	5,385	5,291	3,817	7,330	5,240	4,585
11	2	1	2	2	2	2	7,730	7,550	4,902	9,889	7,607	6,295
12	2	1	3	2	3	3	8,932	8,895	7,111	-	9,053	8,607
13	2	2	1	2	2	2	7,445	7,322	4,998	-	7,179	6,203
14	2	2	2	2	2	2	9,749	9,517	6,170	-	9,318	7,731
15	2	2	3	2	2	3	12,628	12,423	8,367	-	13,841	10,735
16	2	3	1	3	2	2	9,452	9,312	5,886	-	9,007	7,523
17	2	3	2	3	3	2	11,589	11,338	7,262	-	11,099	9,123
18	2	3	3	3	3	3	15,258	15,065	9,636	-	15,010	12,187
19	3	1	1	3	3	1	4,022	4,012	3,778	6,874	4,511	4,149
20	3	1	2	3	3	3	6,598	6,532	5,386	10,290	7,740	6,523
21	3	1	3	3	3	3	8,938	8,919	8,095	10,704	9,416	8,954
22	3	2	1	3	3	2	5,915	5,899	5,198	8,414	6,288	5,967
23	3	2	2	3	3	3	8,422	8,360	6,867	-	9,458	8,220
24	3	2	3	3	3	3	12,130	12,046	9,954	15,321	13,114	11,926
25	3	3	1	3	3	3	8,322	8,261	6,491	-	8,630	7,971
26	3	3	2	3	3	3	10,387	10,285	8,246	-	11,095	9,957
27	3	3	3	3	3	3	14,526	14,399	11,505	-	15,573	13,989
28	4	1	1	4	4	1	-	-	-	-	-	-
29	4	1	2	4	4	2	-	-	-	-	-	-
30	4	1	3	4	4	3	-	-	-	-	-	-
31	4	2	1	4	4	2	-	-	-	-	-	-
32	4	2	2	4	4	2	-	-	-	-	-	-
33	4	2	3	4	4	3	-	-	-	-	-	-
34	4	3	1	4	4	3	-	-	-	-	-	-
35	4	3	2	4	4	3	-	-	-	-	-	-
36	4	3	3	4	4	3	-	-	-	-	-	-

A denotes adhesive layer thickness, B denotes adherend thickness and C denotes bond length.

Table B3: Effect of Main Factors on the Strength of CR1 Mild Steel/AV119 Epoxy Single-Lap Joints (von Mises material model)

Main Factor	Predicted Failure Load (N)					
	Maximum Shear Stress	Maximum Tensile Stress	Hill's Failure Criterion	Maximum Shear Strain	Maximum Tensile Strain	Maximum Principal Strain
A_1	7,962 ± 2,200	8,058 ± 2,235	5,070 ± 1,328	10,534 ± 2,459	9,426 ± 2,829	7,399 ± 2,052
A_2	9,121 ± 2,682	9,483 ± 2,785	6,035 ± 1,703	9,769 ± 2,331	9,666 ± 2,995	8,204 ± 2,440
A_3	8,854 ± 3,146	8,999 ± 3,187	6,784 ± 2,290	10,957 ± 3,802	9,395 ± 3,400	8,476 ± 3,042
A_4	6,268 ± 1,928	6,929 ± 2,133	4,798 ± 1,512	9,516 ± 314	6,211 ± 2,041	5,808 ± 1,921
B_1	6,564 ± 2,056	6,704 ± 2,030	4,659 ± 1,461	8,639 ± 1,655	6,911 ± 1,965	6,022 ± 1,820
B_2	8,548 ± 2,333	8,718 ± 2,363	5,920 ± 1,642	10,804 ± 2,377	9,465 ± 2,562	8,019 ± 2,150
B_3	10,112 ± 2,461	10,543 ± 2,372	6,961 ± 1,848	12,282 ± 3,282	11,285 ± 2,826	9,485 ± 2,271
C_1	6,308 ± 1,495	6,622 ± 1,719	4,539 ± 1,056	8,237 ± 1,570	6,715 ± 1,720	5,894 ± 1,473
C_2	8,286 ± 1,560	8,361 ± 1,859	5,518 ± 1,299	10,229 ± 1,879	9,081 ± 1,644	7,510 ± 1,557
C_3	11,330 ± 1,963	11,506 ± 2,027	7,827 ± 1,605	12,957 ± 2,923	12,293 ± 2,640	10,512 ± 1,979

A denotes adhesive layer thickness, B denotes adherend thickness and C denotes bond length.

Table B4: Effect of Interactions on the Strength of CR1 Mild Steel/AV119 Epoxy Single-Lap Joints (von Mises material model)

Main Factor	Predicted Failure Load (N)					
	Maximum Shear Stress	Maximum Tensile Stress	Hill's Failure Criterion	Maximum Shear Strain	Maximum Tensile Strain	Maximum Principal Strain
$(A \times B)_1$	6,548 ± 1,994	6,605 ± 1,986	4,264 ± 1,212	9,262 ± 721	7,269 ± 1,775	6,043 ± 1,811
$(A \times B)_2$	8,234 ± 2,213	8,380 ± 2,254	5,385 ± 1,397	9,915 ± 2,470	8,926 ± 2,427	7,439 ± 2,030
$(A \times B)_3$	9,329 ± 3,075	9,628 ± 3,152	6,857 ± 2,101	10,841 ± 3,603	10,004 ± 3,377	8,818 ± 2,863
$(A \times B)_4$	6,268 ± 1,928	6,929 ± 2,133	4,798 ± 1,512	9,516 ± 314	6,211 ± 2,041	5,808 ± 1,921
$(A \times C)_1$	6,057 ± 1,309	6,125 ± 1,324	3,928 ± 673	8,259 ± 1,030	7,098 ± 1,693	5,679 ± 1,229
$(A \times C)_2$	7,910 ± 1,972	8,144 ± 2,041	5,140 ± 1,241	9,822 ± 2,107	8,788 ± 2,150	7,176 ± 1,807
$(A \times C)_3$	9,616 ± 2,892	9,827 ± 2,977	6,883 ± 1,933	11,375 ± 3,514	10,497 ± 3,396	9,060 ± 2,686
$(A \times C)_4$	6,268 ± 1,928	6,929 ± 2,133	4,798 ± 1,512	9,516 ± 314	6,211 ± 2,041	5,808 ± 1,921
$(B \times C)_1$	4,572 ± 451	4,749 ± 442	4,785 ± 647	7,000 ± 2,087	4,785 ± 649	4,217 ± 335
$(B \times C)_2$	7,523 ± 1,360	7,810 ± 1,566	8,353 ± 1,718	9,267 ± 1,324	8,353 ± 1,718	6,882 ± 1,239
$(B \times C)_3$	9,708 ± 2,701	9,931 ± 2,734	10,517 ± 3,120	11,560 ± 3,211	10,517 ± 3,120	9,092 ± 2,501

A denotes adhesive layer thickness, B denotes adherend thickness and C denotes bond length.

Table B5: Effect of Main Factors on the Strength of CR1 Mild Steel/AV119 Epoxy Single-Lap Joints (Linear Drucker-Prager material model)

Main Factor	Predicted Failure Load (N)					
	Maximum Shear Stress	Maximum Tensile Stress	Hill's Failure Criterion	Maximum Shear Strain	Maximum Tensile Strain	Maximum Principal Strain
A_1	8,278 ± 2,736	8,144 ± 2,560	5,396 ± 1,545	9,364 ± 2,750	9,233 ± 3,131	7,161 ± 1,938
A_2	9,796 ± 2,983	9,635 ± 2,945	6,461 ± 1,823	8,610 ± 1,809	9,904 ± 3,170	8,110 ± 2,362
A_3	8,777 ± 3,158	8,746 ± 3,183	7,280 ± 2,439	10,321 ± 3,188	9,536 ± 3,383	8,628 ± 3,034
A_4	-	-	-	-	-	-
B_1	6,885 ± 1,869	6,829 ± 1,864	5,207 ± 1,608	8,814 ± 1,717	7,264 ± 1,819	6,313 ± 1,833
B_2	9,215 ± 2,834	9,017 ± 2,670	6,376 ± 1,945	11,282 ± 3,748	9,939 ± 2,797	8,048 ± 735
B_3	10,751 ± 2,766	10,678 ± 2,763	7,554 ± 2,054	-	12,111 ± 2,865	9,539 ± 2,388
C_1	6,482 ± 1,749	6,413 ± 1,719	4,681 ± 1,092	7,349 ± 802	6,657 ± 1,619	5,888 ± 1,368
C_2	8,585 ± 1,667	8,478 ± 1,618	6,033 ± 1,255	9,728 ± 658	9,337 ± 1,613	7,568 ± 1,418
C_3	11,784 ± 2,407	11,634 ± 2,345	8,422 ± 1,687	12,428 ± 2,465	12,405 ± 2,630	10,443 ± 1,922

A denotes adhesive layer thickness, B denotes adherend thickness and C denotes bond length.

Table B6: Effect of Interactions on the Strength of CR1 Mild Steel/AV119 Epoxy Single-Lap Joints (Linear Drucker-Prager material model)

Main Factor	Predicted Failure Load (N)					
	Maximum Shear Stress	Maximum Tensile Stress	Hill's Failure Criterion	Maximum Shear Strain	Maximum Tensile Strain	Maximum Principal Strain
$(A \times B)_1$	6,786 ± 2,033	6,755 ± 2,030	4,591 ± 1,321	8,475 ± 850	7,268 ± 1,820	5,901 ± 1,793
$(A \times B)_2$	8,724 ± 2,716	8,510 ± 2,536	5,688 ± 1,614	9,653 ± 2,860	9,166 ± 2,781	7,312 ± 1,936
$(A \times B)_3$	9,519 ± 3,105	9,458 ± 3,089	7,151 ± 2,110	10,321 ± 3,188	10,408 ± 3,387	8,773 ± 2,612
$(A \times B)_4$	-	-	-	-	-	-
$(A \times C)_1$	5,932 ± 1,194	5,874 ± 1,191	3,988 ± 850	7,065 ± 1,025	6,199 ± 1,221	5,532 ± 1,174
$(A \times C)_2$	8,734 ± 2,149	8,634 ± 2,130	5,883 ± 1,460	8,741 ± 1,300	9,399 ± 2,917	7,497 ± 1,923
$(A \times C)_3$	9,982 ± 3,269	9,862 ± 3,198	7,397 ± 2,058	10,756 ± 2,892	10,541 ± 3,296	9,040 ± 2,613
$(A \times C)_4$	-	-	-	-	-	-
$(B \times C)_1$	4,703 ± 682	4,660 ± 640	3,683 ± 199	6,848 ± 496	5,029 ± 451	4,346 ± 221
$(B \times C)_2$	8,068 ± 1,778	7,954 ± 1,717	5,342 ± 1,044	8,714 ± 894	8,438 ± 1,751	6,875 ± 1,164
$(B \times C)_3$	10,446 ± 2,780	10,284 ± 2,671	7,489 ± 1,823	12,268 ± 2,192	11,943 ± 2,633	9,323 ± 2,140

A denotes adhesive layer thickness, B denotes adherend thickness and C denotes bond length.

Table C1: FEA Strength Predictions for CR1 Mild Steel/XD4601 Epoxy Scarf Joints (von Mises material model)

Case	Taper Angle (degrees)	Adhesive Thickness (mm)	Width (mm)	Predicted Failure Load (N)					
				Maximum Shear Stress	Maximum Tensile Stress	Hill's Failure Criterion	Maximum Shear Strain	Maximum Tensile Strain	Maximum Principal Strain
1	25	0.25	25	24,704	22,800	12,358	20,255	19,027	18,366
2	25	0.50	25	23,925	18,190	12,256	21,016	20,045	19,356
3	25	1.00	25	24,023	17,721	11,326	20,607	19,507	16,761
4	45	0.25	25	20,423	16,119	14,188	20,961	16,534	16,532
5	45	0.50	25	20,434	16,139	13,890	20,849	16,986	16,986
6	45	1.00	25	20,250	16,070	13,585	20,949	16,966	16,965
7	60	0.25	25	22,254	17,934	17,491	22,065	18,820	18,659
8	60	0.50	25	21,563	17,454	15,879	21,448	18,403	18,233
9	60	1.00	25	21,099	16,855	14,890	22,999	18,141	17,937
10	25	0.25	100	193315	146,062	99,739	223,120	170,020	153,885
11	45	0.25	100	164747	129,130	113,675	171,580	166,915	135,971
12	60	0.25	200	178,031	143,476	139,930	195,220	176,517	150,564

Table C2: FEA Strength Predictions for CR1 Mild Steel/XD4601 Epoxy Scarf Joints (Linear Drucker-Prager material model)

Case	Taper Angle (degrees)	Adhesive Thickness (mm)	Width (mm)	Predicted Failure Load (N)					
				Maximum Shear Stress	Maximum Tensile Stress	Hill's Failure Criterion	Maximum Shear Strain	Maximum Tensile Strain	Maximum Principal Strain
1	25	0.25	25	-	16,092	12,547	16,280	14,308	14,026
2	25	0.25	25	18924	16,037	12,353	16,096	14,205	14,110
3	25	0.25	25	19,115	16,120	11,752	15,992	14,388	14,326
4	45	0.50	25	19,296	15,607	14,671	-	15,292	15,270
5	45	0.50	25	18,362	15,350	14,392	19,725	15,394	15,381
6	45	0.50	25	17,782	15,018	14,167	-	15,259	15,244
7	60	1.00	25	22,623	17,643	20,531	21,789	20,626	19,446
8	60	1.00	25	21,749	17,247	18,872	21,503	19,746	19,359
9	60	1.00	25	20,498	16,245	16,666	21,014	19,367	18,958

Table C3: FEA Strength Predictions for CR1 Mild Steel/AV119 Epoxy Scarf Joints (von Mises material model)

Case	Taper Angle (degrees)	Adhesive Thickness (mm)	Width (mm)	Predicted Failure Load (N)					
				Maximum Shear Stress	Maximum Tensile Stress	Hill's Failure Criterion	Maximum Shear Strain	Maximum Tensile Strain	Maximum Principal Strain
1	25	0.25	25	25,533	25,676	14,751	25,768	19,552	18,942
2	45	0.25	25	20,440	20,566	17,465	-	16,940	16,937
3	60	0.25	25	22,771	23,426	21,269	-	23,226	23,150

Table C4: FEA Strength Predictions for CR1 Mild Steel/AV119 Epoxy Scarf Joints (Linear Drucker-Prager material model)

Case	Taper Angle (degrees)	Adhesive Thickness (mm)	Width (mm)	Predicted Failure Load (N)					
				Maximum Shear Stress	Maximum Tensile Stress	Hill's Failure Criterion	Maximum Shear Strain	Maximum Tensile Strain	Maximum Principal Strain
1	25	0.25	25	-	-	15,391	19,478	17,390	17,332
2	45	0.25	25	19,381	19,344	18,449	-	18,033	18,017
3	60	0.25	25	22,212	22,144	23,366	24,646	22,138	20,477

Table D1: Full Matrix of FEA Simulations for Strength Predictions for Mild Steel/XD4601 Epoxy Scarf Joints (von Mises material model)

Runs	Main Factors		Interactions						
	A	B	A x B	Maximum Shear Stress	Maximum Tensile Stress	Hill's Failure Criterion	Maximum Shear Strain	Maximum Tensile Strain	Maximum Principal Strain
1	1	1	1	24,704	22,800	12,358	20,255	19,027	18,366
2	1	2	2	23,925	18,190	12,256	21,016	20,045	19,356
3	1	3	3	24,023	17,721	11,326	20,607	19,507	16,761
4	2	1	2	20,423	16,119	14,188	20,961	16,534	16,532
5	2	2	2	20,434	16,139	13,890	20,849	16,986	16,986
6	2	3	3	20,250	16,070	13,585	20,949	16,966	16,965
7	3	1	3	22,254	17,934	17,491	22,065	18,820	18,659
8	3	2	3	21,563	17,454	15,879	21,448	18,403	18,233
9	3	3	3	21,099	16,855	14,890	22,999	18,141	17,937

A denotes taper angle and B denotes adhesive layer thickness.

Table D2: Full Matrix of FEA Simulations for Strength Predictions for Mild Steel/XD4601 Epoxy Scarf Joints (Linear Drucker-Prager material model)

Runs	Main Factors		Interactions						
	A	B	A x B	Maximum Shear Stress	Maximum Tensile Stress	Hill's Failure Criterion	Maximum Shear Strain	Maximum Tensile Strain	Maximum Principal Strain
1	1	1	1	-	16,092	12,547	16,280	14,308	14,026
2	1	2	2	18924	16,037	12,353	16,096	14,205	14,110
3	1	3	3	19,115	16,120	11,752	15,992	14,388	14,326
4	2	1	2	19,296	15,607	14,671	-	15,292	15,270
5	2	2	2	18,362	15,350	14,392	19,725	15,394	15,381
6	2	3	3	17,782	15,018	14,167	-	15,259	15,244
7	3	1	3	22,623	17,643	20,531	21,789	20,626	19,446
8	3	2	3	21,749	17,247	18,872	21,503	19,746	19,359
9	3	3	3	20,498	16,245	16,666	21,014	19,367	18,958

A denotes taper angle and B denotes adhesive layer thickness.

Table D3: Effect of Main Factors on the Strength of Mild Steel/ XD4601 Epoxy Scarf Joints (von Mises material model)

Main Factor	Predicted Failure Load (N)					
	Maximum Shear Stress	Maximum Tensile Stress	Hill's Failure Criterion	Maximum Shear Strain	Maximum Tensile Strain	Maximum Principal Strain
A_1	24,217 ± 424	19,570 ± 2,806	11,980 ± 569	20,626 ± 381	19,526 ± 509	18,161 ± 1,310
A_2	20,369 ± 103	16,109 ± 36	13,888 ± 302	20,920 ± 61	16,829 ± 255	16,827 ± 256
A_3	21,639 ± 581	17,414 ± 541	16,087 ± 1,313	22,170 ± 781	18,455 ± 342	18,276 ± 363
B_1	22,460 ± 2,148	18,951 ± 3,455	14,679 ± 2,601	21,094 ± 912	18,127 ± 1,383	17,852 ± 1,153
B_2	21,974 ± 1,781	17,261 ± 1,039	14,008 ± 1,814	21,104 ± 309	18,478 ± 1,531	18,191 ± 1,186
B_3	21,791 ± 1,979	16,882 ± 826	13,267 ± 1,803	21,518 ± 1,294	18,205 ± 1,272	17,221 ± 628

A denotes taper angle and B denotes adhesive layer thickness.

Table D4: Effect of Interactions on the Strength of Mild Steel/ XD4601 Epoxy Scarf Joints (von Mises material model)

Main Factor	Predicted Failure Load (N)					
	Maximum Shear Stress	Maximum Tensile Stress	Hill's Failure Criterion	Maximum Shear Strain	Maximum Tensile Strain	Maximum Principal Strain
$(A \times B)_1$	24,704	22,800	12,358	20,255	19,027	18,366
$(A \times B)_2$	21,594 ± 2,019	16,816 ± 1,190	13,445 ± 1,040	20,942 ± 85	17,855 ± 1,910	17,625 ± 1,516
$(A \times B)_3$	21,838 ± 1,422	17,207 ± 753	14,634 ± 2,336	21,614 ± 949	18,367 ± 938	17,711 ± 819

A denotes taper angle and B denotes adhesive layer thickness.

Table D5: Effect of Main Factors on the Strength of Mild Steel/ XD4601 Epoxy Scarf Joints (Linear Drucker-Prager material model)

Main Factor	Predicted Failure Load (N)					
	Maximum Shear Stress	Maximum Tensile Stress	Hill's Failure Criterion	Maximum Shear Strain	Maximum Tensile Strain	Maximum Principal Strain
A_1	19,020 ± 135	16,083 ± 42	12,217 ± 414	16,122 ± 146	14,300 ± 92	14,154 ± 155
A_2	18,480 ± 764	15,325 ± 295	14,410 ± 252	19,275	15,315 ± 70	15,298 ± 73
A_3	21,623 ± 1,068	17,045 ± 720	18,690 ± 1,939	21,435 ± 392	19,913 ± 646	19,254 ± 260
B_1	20,960 ± 2,353	16,447 ± 1,063	15,917 ± 4,135	19,035 ± 3,895	16,742 ± 3,399	16,247 ± 2,839
B_2	19,678 ± 1,815	16,211 ± 960	15,206 ± 3,335	19,108 ± 2,756	16,448 ± 2,917	16,283 ± 2,738
B_3	19,132 ± 1,358	15,794 ± 675	14,195 ± 2,457	18,503 ± 3,551	16,338 ± 2,659	16,176 ± 2,453

A denotes taper angle and B denotes adhesive layer thickness.

Table D6: Effect of Interactions on the Strength of Mild Steel/ XD4601 Epoxy Scarf Joints (Linear Drucker-Prager material model)

Main Factor	Predicted Failure Load (N)					
	Maximum Shear Stress	Maximum Tensile Stress	Hill's Failure Criterion	Maximum Shear Strain	Maximum Tensile Strain	Maximum Principal Strain
$(A \times B)_1$	-	16,092	12,547	16,280	14,308	14,026
$(A \times B)_2$	18,861 ± 470	15,665 ± 347	13,805 ± 1,265	17,911 ± 2,566	14,963 ± 659	14,920 ± 704
$(A \times B)_3$	20,353 ± 1,954	16,455 ± 1,032	16,398 ± 3,530	20,075 ± 2740	17,877 ± 2,842	17,466 ± 2,476

A denotes taper angle and B denotes adhesive layer thickness.